


# Rapid evolution and transformation into quiescence?: ALMA view on $z > 6$ low-luminosity quasars

Takuma Izumi<sup>1,2</sup> , Masafusa Onoue<sup>3</sup>, Yoshiki Matsuoka<sup>4</sup>,  
Tohru Nagao<sup>4</sup>, Michael A. Strauss<sup>5</sup>, Masatoshi Imanishi<sup>1,2</sup>,  
Nobunari Kashikawa<sup>6</sup>, Seiji Fujimoto<sup>7</sup>, Kotaro Kohno<sup>8</sup>,  
Yoshiki Toba<sup>9,4</sup>, Hideki Umehata<sup>10,8</sup>, Tomotsugu Goto<sup>11</sup>,  
Yoshihiro Ueda<sup>9</sup>, Hikari Shirakata<sup>12</sup>, John D. Silverman<sup>13</sup>,  
Jenny E. Greene<sup>14</sup>, Yuichi Harikane<sup>7</sup>, Yasuhiro Hashimoto<sup>15</sup>,  
Soh Ikarashi<sup>16</sup>, Daisuke Iono<sup>1,2</sup>, Kazushi Iwasawa<sup>17</sup>, Chien-Hsiu Lee<sup>1</sup>,  
Takeo Minezaki<sup>8</sup>, Kouichiro Nakanishi<sup>1,2</sup>, Yoichi Tamura<sup>18</sup>,  
Ji-Jia Tang<sup>19</sup> and Akio Taniguchi<sup>18</sup>

<sup>1</sup>National Astronomical Observatory of Japan, Mitaka, Tokyo, 181-8588 Japan  
email: [takuma.izumi@nao.ac.jp](mailto:takuma.izumi@nao.ac.jp)

<sup>2</sup>Department of Astronomical Science, SOKENDAI, Mitaka, Tokyo, Japan

<sup>3</sup>Max Planck Institut für Astronomie, Königstuhl 17, D-69117 Heidelberg, Germany

<sup>4</sup>Research Center for Space and Cosmic Evolution, Ehime University, Ehime, Japan

<sup>5</sup>Princeton University Observatory, Peyton Hall, Princeton, NJ 08544, USA

<sup>6</sup>Department of Astronomy, School of Science, The University of Tokyo, Tokyo, Japan

<sup>7</sup>Institute for Cosmic Ray Research, The University of Tokyo, Chiba, Japan

<sup>8</sup>Institute of Astronomy, Graduate School of Science, The University of Tokyo, Tokyo, Japan

<sup>9</sup>Department of Astronomy, Kyoto University, Kyoto, Japan

<sup>10</sup>RIKEN Cluster for Pioneering Research, Saitama, Japan

<sup>11</sup>Institute of Astronomy and Department of Physics, National Tsing Hua University, Taiwan

<sup>12</sup>Department of CosmoSciences, Hokkaido University, Hokkaido, Japan

<sup>13</sup>Kavli Institute for the Physics and Mathematics of the Universe, Chiba, Japan

<sup>14</sup>Department of Astrophysics, Princeton University, Princeton, NJ, USA

<sup>15</sup>Department of Earth Sciences, National Taiwan Normal University, Taipei, Taiwan

<sup>16</sup>Kapteyn Astronomical Institute, University of Groningen, Groningen, Netherlands

<sup>17</sup>ICREA and Institut de Ciències del Cosmos, Universitat de Barcelona, Barcelona, Spain

<sup>18</sup>Division of Particle and Astrophysical Science, Nagoya University, Aichi, Japan

<sup>19</sup>Australian National University, Weston Creek, Australia

**Abstract.** We present ALMA [CII] line and far-infrared (FIR) continuum observations of seven  $z > 6$  low-luminosity quasars ( $M_{1450} > -25$  mag) discovered by our on-going Subaru Hyper Suprime-Cam survey. The [CII] line was detected in all targets with luminosities of  $\sim (2 - 10) \times 10^8 L_{\odot}$ , about one order of magnitude smaller than optically luminous quasars. Also found was a wide scatter of FIR continuum luminosity, ranging from  $L_{\text{FIR}} < 10^{11} L_{\odot}$  to  $\sim 2 \times 10^{12} L_{\odot}$ . With the [CII]-based dynamical mass, we suggest that a significant fraction of low-luminosity quasars are located on or even below the local Magorrian relation, particularly at the massive end of the galaxy mass distribution. This is a clear contrast to the previous finding that luminous quasars tend to have overmassive black holes relative to the relation. Our result is expected to show a less-biased nature of the early co-evolution of black holes and their host galaxies.

**Keywords.** quasars: general, galaxies: evolution, galaxies: high-redshift

## 1. Introduction

In the local universe, it is clear that the mass of a supermassive black hole (SMBH) is tightly correlated with that of a spheroidal component of its host galaxy (e.g., [Kormendy & Ho 2013](#)). This relation, as well as the remarkable similarity between global star formation and SMBH mass accretion histories (e.g., [Madau & Dickinson 2014](#)), suggest that black holes and their host galaxies have *co-evolved*. Postulated physical mechanisms of co-evolution include mergers of galaxies and feedback of active galactic nuclei (AGN) to terminate star formation in the host (e.g., [Di Matteo \*et al.\* 2005](#); [Hopkins \*et al.\* 2008](#)).

Observations of physical properties of both SMBHs and their host galaxies over cosmic time are essential to test such models, as they specifically predict time evolution of the systems (e.g., [Gallerani \*et al.\* 2017](#)). High redshift quasars provide the unique sites for this purpose. Indeed, the last two decades have witnessed the discovery of  $> 200$  quasars at  $z > 5.7$  owing to wide-field optical and near-infrared (NIR) surveys like the Sloan Digital Sky Survey (SDSS; e.g., [Fan \*et al.\* 2003](#); [Jiang \*et al.\* 2016](#)). These quasars are luminous at optical ( $M_{1450} < -25$  mag), with SMBH masses of  $M_{\text{BH}} \gtrsim 10^9 M_{\odot}$  (e.g., [De Rosa \*et al.\* 2014](#)). Far-infrared (FIR) to submillimeter observations of cool interstellar medium have provided crucial information of their host galaxies as they are hard to detect at rest-frame ultraviolet-to-optical wavelength, due to the outshining quasar nuclei. These host galaxies typically possess copious amount of dust ( $M_{\text{dust}} \gtrsim 10^8 M_{\odot}$ ) and gas ( $M_{\text{H}_2} \gtrsim 10^{10} M_{\odot}$ ), with FIR continuum-based star formation rate (SFR) of  $\gtrsim 100 - 1000 M_{\odot} \text{ yr}^{-1}$  (e.g., [Wang \*et al.\* 2011a,b](#)). The dusty starburst regions appear to be compact, with sizes of a few kpc or less (e.g., [Venemans \*et al.\* 2016](#)).

Recent high resolution submillimeter observations by the Atacama Large Millimeter/submillimeter Array (ALMA) have provided detailed properties of the high redshift quasar host galaxies, including their dynamical masses measured via [CII] emission line. They have found that  $z \gtrsim 6$  luminous quasars have ratios of  $M_{\text{BH}}$  to host galaxy dynamical mass ( $M_{\text{dyn}}$ )  $\sim 10$  times larger than the  $z \sim 0$  relation (e.g., [Wang \*et al.\* 2013](#); [Venemans \*et al.\* 2016](#)) if we equate  $M_{\text{dyn}}$  to the bulge mass ( $M_{\text{bulge}}$ ). However, there is an observational bias, whereby more luminous quasars are powered by more massive SMBHs at high redshifts ([Lauer \*et al.\* 2007](#)). Indeed, early observations of low-luminosity ( $M_{1450} \gtrsim -25$  mag) quasars showed that they are powered by less massive SMBHs ( $\sim 10^8 M_{\odot}$ ), and showed  $M_{\text{BH}}/M_{\text{dyn}}$  (surrogate of  $M_{\text{BH}}/M_{\text{bulge}}$ ) ratios roughly consistent with local galaxies (e.g., [Willott \*et al.\* 2015, 2017](#)).

With this in mind, we have been conducting ALMA observations toward optically low-luminosity quasars, originally discovered by our on-going optical survey with the Subaru Hyper Suprime-Cam (HSC): we have thus far discovered  $> 80$  low-luminosity quasar at  $z \gtrsim 6$  down to  $M_{1450} \sim -22$  mag ([Matsuoka \*et al.\* 2016, 2018a,b](#)). We then organized an intensive multi-wavelength follow-up consortium: *Subaru High- $z$  Exploration of Low-Luminosity Quasars (SHELLQs)*. Here we present an overview of our ALMA programs.

## 2. ALMA Observations and Data Analysis

We have observed [CII] 158  $\mu\text{m}$  line and the underlying rest-FIR continuum emission toward seven  $z \gtrsim 6$  HSC quasars in ALMA Cycle 4 (4 objects) and Cycle 5 (3 objects), respectively ([Izumi \*et al.\* 2018, 2019](#)). The band 6 receiver was used to cover the redshifted [CII] line at  $\sim 230$  GHz. During the observations, 40–47 antennas were available and the range of baseline lengths was between 15–784 m, which resulted in a good  $uv$  coverage

**Table 1.** Overview of the HSC quasars observed by ALMA.

Name	$z_{\text{[CII]}}$	$M_{1450}$ (mag)	$M_{\text{BH}}$ ( $M_{\odot}$ )	$L_{\text{[CII]}}$ ( $10^8 L_{\odot}$ )	$L_{\text{FIR}}$ ( $10^{11} L_{\odot}$ )	SFR ( $M_{\odot} \text{ yr}^{-1}$ )	$M_{\text{dyn}}$ ( $10^{10} M_{\odot}$ )
J0859+0022	6.3903	-24.1	0.3	$4.6 \pm 0.5$	$3.4 \pm 0.5$	$71 \pm 10$	5.6
J1152+0055	6.3637	-25.3	6.3	$3.8 \pm 0.8$	$4.1 \pm 0.7$	$86 \pm 14$	1.4
J2216-0016	6.0962	-23.8	7.0	$10.2 \pm 0.8$	$2.8 \pm 0.6$	$58 \pm 11$	8.2
J1202-0057	5.9289	-22.8	$> 0.4$	$6.2 \pm 0.4$	$4.8 \pm 0.2$	$100 \pm 5$	4.4
J1208-0200	6.1165	-24.3	7.1	$2.7 \pm 0.5$	$1.6 \pm 0.4$	$34 \pm 8$	1.3
J2228+0152	6.0805	-24.0	$> 1.1$	$2.4 \pm 0.6$	$< 0.9$	$< 20$	2.0
J2239+0207	6.2497	-24.6	11	$9.5 \pm 0.9$	$22 \pm 1$	$453 \pm 10$	29

Notes:  $M_{1450}$  and  $M_{\text{BH}}$  are quoted from Matsuoka *et al.* (2016, 2018a) and Onoue *et al.* 2019. For J1202-0057 and J2228+0152, we assumed the Eddington-limited accretion to compute the lower-limit of their  $M_{\text{BH}}$ .

and a typical synthesized beam size of  $\sim 0''.5$ . Reduction and calibration of the data were performed with the Common Astronomy Software Applications package (CASA, McMullin *et al.* 2007) in a standard manner. All images were reconstructed with the CASA task `clean`. The typical noise level is  $\sim 0.10 - 0.24 \text{ mJy beam}^{-1}$  for the [CII] cubes, depending on the adopted velocity resolution (50 or 100  $\text{km s}^{-1}$ ). Their [CII] line luminosities ( $L_{\text{[CII]}}$ ) were computed with the standard equation. To derive their FIR continuum luminosities ( $L_{\text{FIR}}$ ), we assumed a modified black body spectrum with a dust temperature of 47 K and an emissivity index of 1.6. These returned  $L_{\text{[CII]}} \simeq (3 - 10) \times 10^8 L_{\odot}$  and  $L_{\text{FIR}} \simeq (1 - 20) \times 10^{11} L_{\odot}$ . The spatial extents of [CII] emitting regions were measured by applying a 2-dimensional Gaussian profile to the velocity-integrated intensity distributions, yielding  $\sim 2 - 3 \text{ kpc FWHM}$  (major axis). Properties of the targets are listed in Table 1.

### 3. Results and Discussion

*Dynamical mass ( $M_{\text{dyn}}$ ).* We measured  $M_{\text{dyn}}$  of our HSC quasar host galaxies based on their [CII] spatial extents and FWHM, and by following the standard procedure described in Wang *et al.* (2010). The resultant values are listed in Table 1, but formal errors are omitted as there are multiple *unconstrained* uncertainties including the inclination angles and the true geometry of the line emitting region. Despite those uncertainties, we use  $M_{\text{dyn}}$  as a surrogate for  $M_{\text{bulge}}$  (e.g., Wang *et al.* 2013; Venemans *et al.* 2016). As seen in other  $z \gtrsim 6$  quasars,  $M_{\text{dyn}}$  of our low-luminosity HSC quasars exceed  $10^{10} M_{\odot}$ , or even  $10^{11} M_{\odot}$ , which lie at the massive end of the stellar mass distribution for  $z \sim 6$  galaxies in general (e.g., Grazian *et al.* 2015). Therefore, the host galaxies of these HSC quasars are among the most evolved systems known to date at  $z \sim 6$ .

*Comparison with the star-forming main sequence.* We estimated star formation rates (SFR) of our HSC quasars based on their total infrared (TIR; 8–1000  $\mu\text{m}$ ) luminosities, which were computed by assuming the same modified black body profile as described in § 2. The calibration of Murphy *et al.* (2011),  $SFR/M_{\odot} \text{ yr}^{-1} = 1.49 \times 10^{-10} L_{\text{TIR}}/L_{\odot}$ , was applied for this purpose. The resultant values span over a wide range, from  $< 20 M_{\odot} \text{ yr}^{-1}$  to  $\sim 450 M_{\odot} \text{ yr}^{-1}$ . The same calibration was applied to some other  $z \gtrsim 6$  quasars known to date, which are compiled from the literature (see details in Izumi *et al.* 2018, 2019). By equating the [CII]-based  $M_{\text{dyn}}$  to stellar mass of the host galaxies, we can place these  $z \gtrsim 6$  quasars on the  $M_{\text{star}}$ -SFR plane (Figure 1). Our particular interest is paid on the comparison of these quasars with the  $z \sim 6$  star-forming main sequence (MS; Salmon *et al.* 2015). Figure 1 suggests that, while optically-luminous quasars show *starburst* class SFR on this plane (i.e., above the MS), low-luminosity quasars including our HSC quasars are located on or even below the MS. This would indicate that these low-luminosity quasars are transforming into a quiescent population.

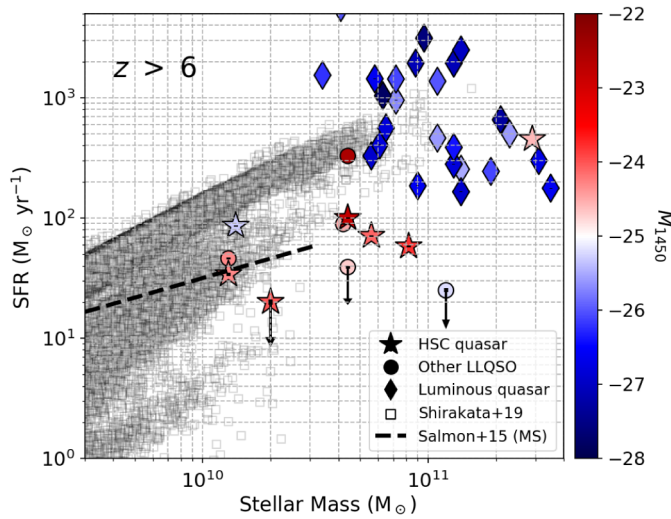


**Figure 1.** SFR plotted as a function of stellar mass (updated from Izumi *et al.* 2018). The dashed line indicates the star-forming main sequence (MS) for  $z \sim 6$  galaxies (Salmon *et al.* 2015). Background gray squares show simulated  $z \sim 6$  galaxies based on our semi-analytic model ( $\nu^2$ GC model; Shirakata *et al.* 2019), which show two sequences: MS and starburst sequence. By equating  $M_{\text{dyn}}$  to stellar mass, we plot  $z > 6$  quasars, which are color-coded by their  $M_{1450}$ . Many of the HSC quasars are located on or even below the MS, suggesting that they are transforming into a quiescent population.

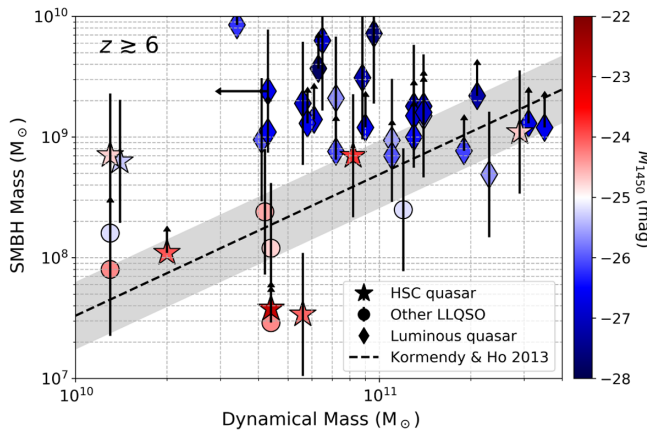


**Figure 2.** Black hole mass ( $M_{\text{BH}}$ ) vs host galaxy dynamical mass ( $M_{\text{dyn}}$ ) relationship for  $z \gtrsim 6$  quasars, color-coded by their  $M_{1450}$  magnitude (Izumi *et al.* 2019). The diagonal dashed line and the shaded region indicate the local  $M_{\text{BH}} - M_{\text{bulge}}$  relationship and its  $1\sigma$  scatter, respectively (Kormendy & Ho 2013). It is clear that optically luminous quasars ( $M_{1450} \lesssim -25$  mag) typically show overmassive  $M_{\text{BH}}$  relative to the local relation, whereas low-luminosity quasars lie close to, or even below, that relation.

*Less-biased early co-evolution.* We also compiled MgII-based (i.e., single-epoch method)  $M_{\text{BH}}$  data and/or  $M_{1450}$  data of  $z \gtrsim 6$  quasars known to date from the literature (see details in Izumi *et al.* 2019). The latter data is used to compute the lower-limit of  $M_{\text{BH}}$  by assuming the Eddington-limited mass accretion. The total number of the quasars compiled here is 40. The  $M_{\text{BH}}$  measurements of our HSC quasars, which are also based on the single-epoch method with MgII line, are described in Onoue *et al.* (2019).

In Figure 2 we display the relation between  $M_{\text{BH}}$  and  $M_{\text{dyn}}$  for the above-mentioned quasars, overlaid with the local  $M_{\text{BH}} - M_{\text{bulge}}$  relation after equating  $M_{\text{dyn}}$  to  $M_{\text{bulge}}$  (Kormendy & Ho 2013). Regarding the optically luminous quasars ( $M_{1450} \lesssim -25$  mag), this figure supports conclusions in previous works (e.g., Wang *et al.* 2013; Venemans *et al.* 2016), i.e., the luminous quasars typically have overmassive SMBHs relative to the local relation, although the discrepancy becomes less evident at  $M_{\text{dyn}} \gtrsim 10^{11} M_{\odot}$ . On the other hand, most of the low-luminosity quasars ( $M_{1450} \gtrsim -25$  mag) show comparable ratios to, or even lower ratios than, the local relation. The existence of the undermassive SMBHs even implies an evolutionary path, in which galaxies grow earlier than SMBHs, such as expected in a standard merger-induced evolution model (Hopkins *et al.* 2008).

Particularly at a high-mass range ( $M_{\text{dyn}} \gtrsim 4 \times 10^{10} M_{\odot}$ ), our result demonstrates that previous works on luminous quasars have been largely biased toward the most massive SMBHs, easily resulting in objects lying above the local relation. Therefore, our results highlights the power of the sensitive Subaru HSC survey, as well as the importance of probing their host galaxy nature, in order to depict the less-biased, more genuine shape of early co-evolution of SMBHs and galaxies.

## References

- De Rosa, G. *et al.* 2014, *ApJ*, 790, 145  
 Di Matteo, T., Springel, V., & Hernquist, L. 2005, *Nature*, 433, 604  
 Fan, X. *et al.* 2003, *AJ*, 125, 1649  
 Gallerani, S., Fan, X., Maiolino, R., & Pacucci, F. 2017, *PASA*, 34, e022  
 Grazian, A. *et al.* 2015, *A&A*, 575, A96  
 Hopkins, P. F., Hernquist, L., Cox, T. J., & Kereš, D. 2008, *ApJS*, 175, 356  
 Izumi, T. *et al.* 2018, *PASJ*, 70, 36  
 Izumi, T. *et al.* 2019, *PASJ*, in press  
 Jiang, L. *et al.* 2016, *ApJ*, 833, 222  
 Kormendy, J. & Ho, L. C. 2013, *ARAA*, 51, 511  
 Lauer, T. R., Tremaine, S., Richstone, D., & Faber, S. M. 2007, *ApJ*, 670, 249  
 Madau, P. & Dickinson, M. 2014, *ARAA*, 52, 415  
 Matsuoka, Y. *et al.* 2016, *ApJ*, 828, 26  
 Matsuoka, Y. *et al.* 2018a, *PASJ*, 70, S35  
 Matsuoka, Y. *et al.* 2018b, *PASJ*, 237, 5  
 McMullin, J. P., Waters, B., Schiebel, D., Young, W., & Golap, K. 2007, in *ASP Conf. Ser.* 376, Astronomical Data Analysis Software and Systems XVI, ed. R. A. Shaw, F. Hill, & D. J. Bell (San Francisco, CA: ASP), 127  
 Murphy, E. J. *et al.* 2011, *ApJ*, 737, 67  
 Onoue, M. *et al.* 2019, *ApJ*, 880, 77  
 Salmon, B. *et al.* 2015, *ApJ*, 799, 183  
 Shirakata, H. *et al.* 2019, *MNRAS*, 482, 4846  
 Venemans, B. P., Walter, F., Zschaechner, L., Decarli, R., De Rosa, G., Findlay, J. R., McMahon, R. G., & Sutherland, W. J. 2016, *ApJ*, 816, 37  
 Wang, R. *et al.* 2011a, *AJ*, 142, 101  
 Wang, R. *et al.* 2011b, *ApJ*, 739, 34  
 Wang, R. *et al.* 2013, *ApJ*, 773, 44  
 Willott, C. J., Bergeron, J., & Omont, A. 2015, *ApJ*, 801, 123  
 Willott, C. J., Bergeron, J., & Omont, A. 2017, *ApJ*, 850, 108